

Quantum Chemical Modelling of Water Splitting: From Photoelectrochemistry to Superlubricity

L. Mayrhofer, G. Moras, T. Kuwahara, A. Held, M. Moseler

published in

NIC Symposium 2020

M. Müller, K. Binder, A. Trautmann (Editors)

Forschungszentrum Jülich GmbH,
John von Neumann Institute for Computing (NIC),
Schriften des Forschungszentrums Jülich, NIC Series, Vol. 50,
ISBN 978-3-95806-443-0, pp. 75.
<http://hdl.handle.net/2128/24435>

© 2020 by Forschungszentrum Jülich

Permission to make digital or hard copies of portions of this work for personal or classroom use is granted provided that the copies are not made or distributed for profit or commercial advantage and that copies bear this notice and the full citation on the first page. To copy otherwise requires prior specific permission by the publisher mentioned above.

Quantum Chemical Modelling of Water Splitting: From Photoelectrochemistry to Superlubricity

Leonhard Mayrhofer¹, Gianpietro Moras¹, Takuya Kuwahara¹, Alexander Held^{1,2},
and Michael Moseler^{1,2,3}

¹ Fraunhofer IWM, MicroTribology Center μ TC, Wöhlerstr. 11, 79108 Freiburg, Germany
E-mail: {leonhard.mayrhofer, gianpietro.moras, takuya.kuwahara,
michael.moseler}@iwm.fraunhofer.de

² Freiburg Materials Research Center FMF, University of Freiburg,
Stefan-Meier-Straße 21, 79104 Freiburg, Germany

³ Physics Department, University of Freiburg, Hermann-Herder-Str. 3, 79104 Freiburg, Germany

Within the project the electronic structure and chemical reactions at interfaces are investigated by using the quantum chemical methods density functional theory (DFT) and density-functional tight binding (DFTB). The research covers a broad spectrum of topics ranging from sustainable energy materials for solar hydrogen production to the wear and friction in tribological contacts including mechanically induced chemical reactions of lubricant and additive molecules at surfaces. A common feature of the different studies are surface reactions of molecules induced by different driving forces such as excited charge carriers or external mechanical load. Here, selected examples of our studies are presented where the splitting of water molecules at surfaces and interfaces plays a key role. We start with the *ab initio* DFT investigation of unconventional $\text{U}_3\text{O}_8/\text{Fe}_2\text{O}_3$ heterostructures which are used to split water molecules with the purpose of solar hydrogen production and conclude with DFTB simulations of water lubricated carbon coatings where water splitting can lead to extremely low friction, also known as superlubricity.

1 Introduction

Materials play a crucial role for the transition of an economy based on fossil fuels to an economy based on renewable energies. This is also true for a more effective usage of resources by reducing energy consumption and wear of mechanical machinery. Atomistic simulations can help to better understand and predict the microscopic processes determining the functional properties and have thus become a main pillar in materials science. Here, we demonstrate with the aid of two selected examples conducted within this project the abilities of DFT and DFTB simulations to describe systems with very different compositions and functionalities. We first give a short report on our research activities in the field of semiconductor heterostructures for solar water splitting applications and then present a recent study where again water molecule degradation at interfaces is the main concern. However, instead of excited charge carriers, in the second example mechanical load drives the splitting of water or lubricant molecules in tribological contacts of tetrahedral amorphous carbon (ta-C). This induces surface modifications which lead to extremely low friction.

2 Unconventional $\text{U}_3\text{O}_8/\text{Fe}_2\text{O}_3$ Metal Oxide Heterostructures for Water Splitting Applications

Solar energy conversion is a safe, eco-friendly and world's most abundant renewable source of energy. Direct synthesis of chemical fuels like hydrogen by photoconversion processes can overcome the strongly unequal temporal and geographic availability of conventional solar technologies such as photovoltaics. Hydrogen is considered to have a large potential to replace fossil fuels as main primary energy source, which will have a major impact on the global energy systems and the environment.¹ There are various ways of producing solar hydrogen such as, thermo-chemical water splitting, use of photobiological systems, and photoelectrochemical (PEC) water splitting. All pathways can contribute to renewable hydrogen production for future green economies. However, hydrogen generation by PEC reactions is regarded as the "Holy Grail" of the hydrogen economy. PEC water splitting by semiconductor materials is based on a simple principle (Fig. 1): upon photo excitation of an electron-hole pair, the excited electron in the conduction band drives the reduction of water to H_2 , whereas the hole in the valence band oxidises water to O_2 , such that the net effect is the dissociation or splitting of water into gasses of its constituent elements. The minimum theoretical electrical potential required to oxidise water under standard conditions is 1.23 V (vs. a standard hydrogen electrode). However, owing to several factors such as cell resistance, polarisation losses, *etc.* in general an over-potential is needed. As a consequence, the actual voltage required to achieve water electrolysis is typically in the range of 1.8 - 2.0 V. Hence, semiconductor systems with sufficiently large band gaps are required for photoelectrochemical (PEC) water splitting. On the other hand, band gaps far beyond 2 eV only exploit a small part of the solar spectrum for photoelectrolysis and therefore result in low solar energy to hydrogen efficiencies.

In addition to band gap requirements, in total a unique combination of properties has to be satisfied by the employed materials to be well suited for large-scale PEC hydrogen production. The most important are: i) high absorption of solar energy, ii) proper alignment of conduction and valence band edges w.r.t. water redox potentials, iii) long life-time without material degradation and finally iv) earth abundance and low production costs.

So far, no single semiconductor system is known which satisfies all of the mentioned preconditions at the same time. Metal oxides such as Fe_2O_3 or TiO_2 are abundant and stable under PEC conditions but have limitations regarding charge transport properties (Fe_2O_3) or optical absorption in the visible range (TiO_2). Material modifications such as doping or hydrogen treatment processes are one way to enhance the PEC performance of metal oxides and several such approaches were studied theoretically in our group.³⁻⁶ Another approach is the combination of different metal oxides in heterostructure devices, where synergetic effects can drastically increase the PEC performance. Within this project the mechanisms leading to an enhanced water splitting performance of two different metal oxide heterostructures, $\text{BiVO}_4/\text{TiO}_2$ and $\text{U}_3\text{O}_8/\text{Fe}_2\text{O}_3$ were investigated by DFT calculations in collaborative experimental/theoretical studies.^{7,8} The latter study is presented in the following.

The use of uranium oxides for renewable energy conversion might look peculiar on a first glance. However, there is a huge amount of depleted and hence low-radiation uranium available as waste from the nuclear economy.⁹ Due to the problems with the long-term storage of the uranium waste in the form of highly toxic UF_6 , it is highly desirable to find

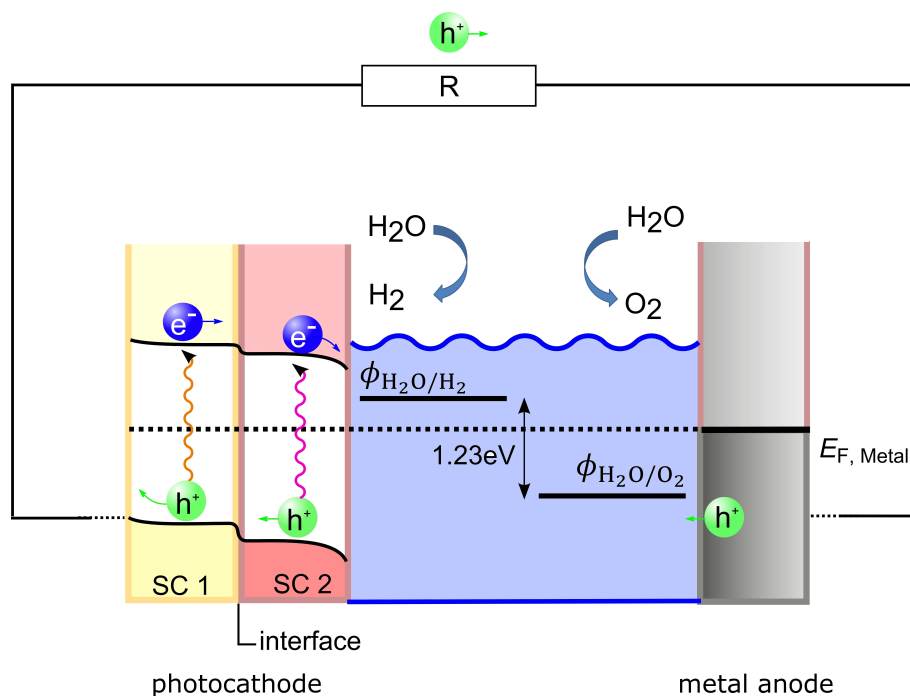


Figure 1. Water splitting is based on the separation of electrons and holes after the photo excitation of electron/hole pairs in semiconductors immersed in an aqueous electrolyte. After photoexcitation and electron-hole separation water molecules can be dissociated if the redox potentials of the water splitting reactions are properly aligned with the semiconductor band edges. The use of semiconductor heterostructures based on two semiconductors with the proper band alignment leads to enhanced electron/hole separation and helps to increase the solar energy to hydrogen conversion efficiencies.

applications of the uranium in a closed environment such that the deconversion of UF_6 to uranium oxide becomes economically viable. Hence, the application of uranium oxides as semiconductors or catalysts has been an active research field over the last twenty years.^{10–13} Together with our experimental partners from the research group of Prof. Sanjay Mathur at the University of Cologne, the properties of $\text{U}_3\text{O}_8/\text{Fe}_2\text{O}_3$ heterostructures as photoanodes for solar water splitting were investigated.⁸ Here, the Fe_2O_3 side of the heterojunction was exposed towards the aqueous electrolyte and supposed to catalyse the water oxidation. Experimentally, a strong enhancement of the PEC performance of $\text{U}_3\text{O}_8/\text{Fe}_2\text{O}_3$ based photoanode was found compared to the conventional PEC material Fe_2O_3 . Pure U_3O_8 even showed negligible photocurrents. Transient absorption spectroscopy (TAS) measurements revealed largely improved charge carrier separation properties of the $\text{U}_3\text{O}_8/\text{Fe}_2\text{O}_3$ heterojunction. Using the DFT+U approach,² extensive simulations of $\text{U}_3\text{O}_8/\text{Fe}_2\text{O}_3$ interfaces were conducted. The calculated interfacial electronic structure revealed a so called type II alignment between the U_3O_8 and Fe_2O_3 band edges which favours the fast separation of electrons and holes, see Fig. 2. The holes favour transport towards the Fe_2O_3 surface to promote the oxidation of water. The electrons are transferred to the counter electrode

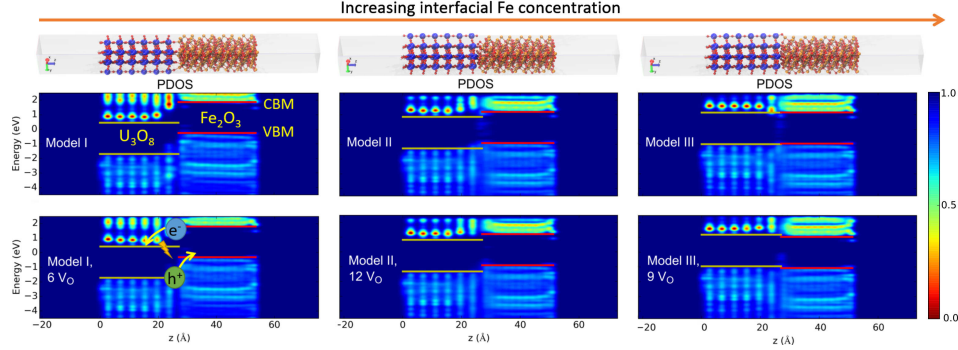


Figure 2. Interfacial electronic structure of different $\text{U}_3\text{O}_8/\text{Fe}_2\text{O}_3$ interface models with varying interfacial Fe and O ion concentration. The projected density of states (PDOS) over the interface shows that the conduction band minimum (CBM) and the valence band maximum (VBM) in Fe_2O_3 are higher than in U_3O_8 except at high interfacial Fe ion concentration and low oxygen concentration (Model III, 9 V_O , where V_O indicates the number of oxygen vacancies in comparison to the original structure). This so called type II alignment favours efficient charge carrier separation of photoexcited electron/hole pairs and leads to enhanced water splitting performance. The atomistic structures of the various interface models are shown on the top. U ions are indicated by blue, Fe ions by brownish and O ions by red spheres. Hydrogen atoms (white spheres) are used to saturate the free U_3O_8 surface. Each interface model contained approximately 700 atoms.

where the actual hydrogen evolution reaction takes place. Interestingly, our simulations revealed that the relative band alignment between Fe_2O_3 and U_3O_8 can be controlled by the concentration of Fe ions at the interface. This behaviour can be traced back to the multivalency of U ions within U_3O_8 . At low enough interfacial concentrations of iron, all Fe ions are in the 3+ state, whereas U_3O_8 intrinsically contains U^{5+} and U^{6+} ions and the 5+ valence state readily switches to the 6+ state due to oxidation by interfacial oxygen species. Hence an interfacial dipole is building up due to charge transfer from O to U ions that tends to lift the Fe_2O_3 electronic states with respect to U_3O_8 . The reverse effect only appears at rather high Fe ion concentrations when also Fe^{2+} ions are present which can be oxidised. Our DFT calculations predicted that high interfacial Fe concentrations are favoured under more reducing conditions and the interesting question arises whether the band alignment can thus be controlled by changing the synthesis conditions. The dependence of the band alignment on the Fe ion concentration could also be quantitatively captured by a simple classical electrostatic model taking into account the valency of the interfacial Fe and U ions and allowed a simple interpretation of the DFT results.

3 Tribochemical Water Splitting for Superlow Friction

The minimisation of frictional losses in mechanical components is of paramount importance to a more efficient use of energy.¹⁴ Very significant reductions of fuel consumption and CO_2 emissions could be achieved by reducing friction in passenger cars to ultralow (friction coefficient μ in the 0.1 – 0.01 range) or even to superlow levels ($\mu < 0.01$).¹⁵ Thanks to the increased scientific effort devoted to this subject in recent years, such extremely low friction levels can be nowadays achieved in tribological systems that are technologically relevant. For instance, in order to optimise the tribological performance of

components that operate under severe environmental or loading conditions, there is an ever increasing use of hard surface coatings made of carbon, both with crystalline (nanocrystalline diamond, NCD) and amorphous (tetrahedral amorphous carbon, ta-C) structure. Not only do these coatings offer very high resistance to wear and corrosion but they can also yield superlow friction coefficients when used in combination with water¹⁶ and other OH-containing molecules, such as hydrogen peroxide or glycerol.¹⁷

Understanding the atomic-scale mechanisms leading to superlow friction is crucial to be able to control the friction behaviour of the system (*e. g.* by introducing the optimal quantity of OH-containing molecules in the system) and to understand whether superlow friction conditions can be transferred to other materials interfaces. However, tribological interfaces are hardly accessible by spectroscopy and microscopy techniques and these have to be used *ex situ*, on surfaces after they have experienced the tribological load. This is why atomistic simulations that can directly “look into” tribologically loaded interfaces are an ideal tool to complement experimental characterisation. Following this concerted approach, and combining experimental and atomistic simulations results,^{16–19} first steps forward were taken towards an explanation of superlubricity of water-lubricated carbon coatings. In vacuum, covalent bonds form between unpassivated diamond or ta-C surfaces. This results in plastic deformation of the interface region through a sp^3 -to- sp^2 rehybridisation^{20–22} and in very high shear stresses, needed to make one surface slide against the other. In presence of water at the sliding interface, tribochemical dissociative chemisorption reactions lead to H/OH-passivation of the carbon surfaces. This prevents the formation of covalent bonds across the sliding interface and results in superlow friction.

In this project, we combined efficient density-functional tight-binding (DFTB) molecular dynamics (MD) and density functional theory (DFT) electronic structure simulations to gain further insights into the mechanisms leading to superlow friction of water-lubricated diamond films.^{23, 24} In particular, our goal was to extend the time scale spanned by previous DFT simulations¹⁹ and to systematically investigate how the quantity of water molecules at the sliding interface can influence such mechanisms. First, we considered the unreconstructed (111) diamond surface, which is the most stable fracture surface and the least prone to amorphisation. We performed sliding MD simulation under a normal load of 5 GPa and a sliding speed of 100 ms^{-1} for water contents that vary from dry sliding conditions to a quantity of water molecules that is larger than the quantity needed to chemically terminate the two surfaces with H atoms and OH groups.

The results of the simulations are summarised in Fig. 3. We observed five different friction regimes that depend on the water quantity. Three of these friction regimes (I, IV and V) are compatible with the conclusions of previous experimental and simulation studies. For dry sliding or very low amounts of water, we observe cold welding and amorphisation of the sliding region with resulting very high friction (friction regime I). If the quantity of water molecules at the sliding interface is sufficient to passivate the two diamond surfaces by dissociative chemisorption, friction can reach ultralow levels, in particular in the case of full passivation of the surface dangling bonds (friction regime IV). The presence of further water leads to the formation of a thin water film between the passivated surfaces with an associated friction coefficient that is higher than in the case of full passivation without water film (friction regime V).

Interestingly, our simulation unveils two friction regimes that were not mentioned in the previous literature (II and III). Despite appearing at the same, low number of water

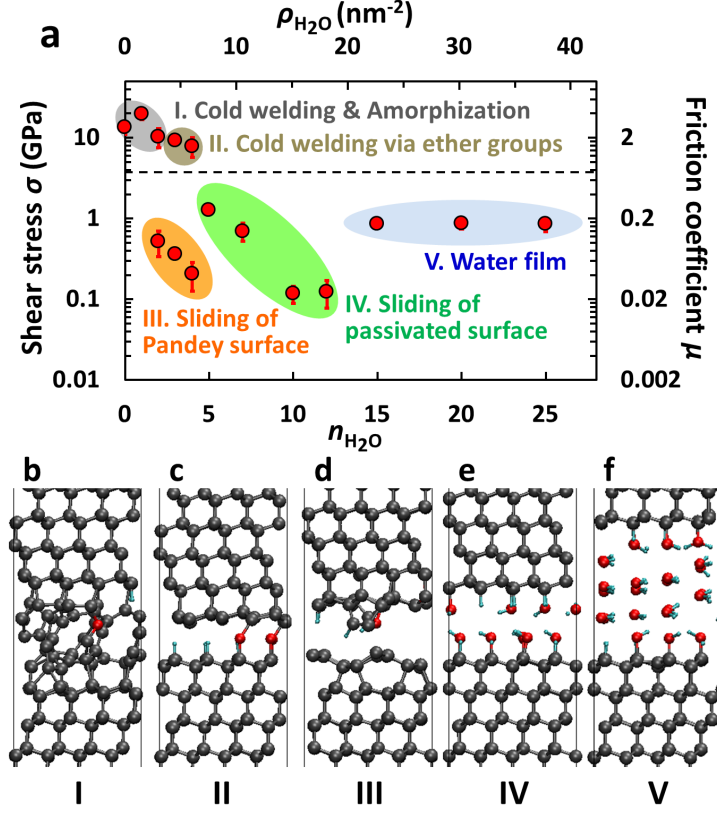


Figure 3. (a) Shear stress σ and friction coefficient μ as a function of the number of water molecules $n_{\text{H}_2\text{O}}$ and of the water surface density $\rho_{\text{H}_2\text{O}}$ for two initially unreconstructed diamond (111) surfaces. Five friction regimes (I-V) are observed. Panels (b) to (f) show representative snapshots for friction regimes I-V. Gray, red and cyan spheres represent carbon, oxygen and hydrogen atoms, respectively. Reused with permission from Ref. 23.

molecules (well below the quantity needed to partially passivate the surfaces), the two friction regimes are characterised by completely different friction coefficients. Friction regime II is obtained when, after tribochemical splitting of the water molecules, ether groups form across the sliding interface which remains crystalline. This is a cold-welding regime with very high friction coefficient. Conversely, friction regime III can potentially lead to super-low friction. After splitting of the water molecules, mechanochemical reactions involving oxygen atoms cause local rearrangements of the surface structure and trigger the reconstruction of one of the diamond surfaces. The surface reconstruction we observe is the so called Pandey reconstruction, which is more stable than the unreconstructed (111) surface when only a few surface dangling bonds are terminated. The aromatic character of the Pandey reconstruction makes it chemically very stable, thus preventing the formation of covalent bonds across the sliding interface.

To understand whether these friction regimes can be found on other crystallographic

orientations of the diamond surface, we adopted the same approach to study the (110) and (100) diamond surfaces.²⁴ We found that the cold-welding regimes I and II, the H/OH-passivation regime IV and the water film regime V are general to all of these low index surfaces. Furthermore, new friction regimes were found on these two crystallographic orientations. Due to the energetic stability of ether and keto groups on the (110) and (100) surfaces, ether- and keto-passivation of these surfaces is possible and can lead to friction coefficients that are very similar to those obtained in regime IV. Moreover, cross-linking ether groups are much less probable at these two interfaces and only give rise to mild cold-welding situations. Finally, superlow friction by aromatic passivation (regime III) was not observed because the (110) and (100) surfaces do not show aromatic reconstructions. However, since an amorphous layer forms on most diamond surfaces after deposition¹⁸ or during tribological load,²⁰ we performed further sliding simulations on ta-C sliding interfaces. The simulations showed that passivating aromatic structures can form on ta-C surfaces in sliding contact with glycerol,²⁵ thus proving the general importance of friction regime III for hard-carbon coatings whenever OH-containing molecules at the sliding interface cannot provide full chemical termination of the surface dangling bonds.

4 Concluding Remarks

We hope that we could convince the reader that water splitting at surfaces and interfaces is a fascinating research topic with a broad range of applications and possibly a large impact on renewable energy conversion and in reducing energy consumption. Quantum chemical methods proved as powerful tools to investigate the mechanisms which drive the water splitting reactions under diverse conditions and for a plethora of different material systems.

Acknowledgements

We gratefully acknowledge the computing time granted by the John von Neumann Institute for Computing (NIC) and provided on the supercomputers JURECA and JUWELS at Jülich Supercomputing Centre (JSC). We feel honoured that our project was selected as John von Neumann Excellence Project 2017. T. K. acknowledges financial support by JSPS Overseas Research Fellowships. A. H. and M. M. are grateful for funding by the Deutsche Forschungsgemeinschaft within Grant No. Mo 879/17. A. H., L. M., and M. M. kindly acknowledge financial support from the Insol Project (BMBF, Grant 01DQ14011) and the SOLAROGENIX Project (EC-FP7-Grant Agreement No. 310333).

References

1. T. Bak, J. Nowotny, M. Rekas, and C. C. Sorrell, *Photo-electrochemical hydrogen generation from water using solar energy. Materials-related aspects*, Int. J. of Hydrogen Energy **27**, 991–1022, 2002.
2. S. L. Dudarev, G. A. Botton, S. Y. Savrasov, C. J. Humphreys, and A. P. Sutton, *Electron-energy-loss spectra and the structural stability of nickel oxide: An LSDA+U study*, Phys. Rev. B **57**, 1505–1509, 1998.

3. M. Mehta, N. Kodan, S. Kumar, A. Kaushal, L. Mayrhofer, M. Walter, M. Moseler, A. Dey, S. Krishnamurthy, S. Basu, and A. P. Singh, *Hydrogen treated anatase TiO₂: a new experimental approach and further insights from theory*, J. Mater. Chem. A **4**, 2670–2681, 2016.
4. A. Mettenbörger, Y. Gönüllü, T. Fischer, T. Heisig, A. Sasinska, C. Maccato, G. Carraro, C. Sada, D. Barreca, L. Mayrhofer, M. Moseler, A. Held, and S. Mathur, *Interfacial insight in multi-junction metal oxide photoanodes for water-splitting applications*, J. Mater. Chem. A **4**, 2670–2681, 2016.
5. D. Primc, G. Zeng, R. Leute, M. Walter, L. Mayrhofer, and M. Niederberger, *Chemical Substitution – Alignment of the Surface Potentials for Efficient Charge Transport in Nanocrystalline TiO₂ Photocatalysts*, Chem. Mater. **28**, 4223–4230, 2016.
6. X. Wang, L. Mayrhofer, M. Höfer, S. Estrade, L. LopezConesa, H. Zhou, Y. Lin, F. Peiró, Z. Fan, H. Shen, L. Schäfer, M. Moseler, G. Bräuer, and A. Waag, *Facile and Efficient Atomic Hydrogenation Enabled Black TiO₂ with Enhanced PhotoElectrochemical Activity via a Favorably Low Energy Barrier Pathway*, Adv. Energy Mater. **9**, 1900725, 2019.
7. A. P. Singh, N. Kodan, B. R. Mehta, A. Held, L. Mayrhofer, and M. Moseler, *Band Edge Engineering in BiVO₄/TiO₂ Heterostructure: Enhanced Photoelectrochemical Performance through Improved Charge Transfer*, ACS Catal. **6**, 5311–5318, 2016.
8. J. Leduc, Y. Gönüllü, T.-P. Ruoko, Th. Fischer, L. Mayrhofer, N. Tkachenko, C. L. Dong, A. Held, M. Moseler, and S. Mathur, *Electronically Coupled Uranium and Iron Oxide Heterojunctions as Efficient Water Oxidation Catalysts*, Adv. Funct. Mater. **29**, forthcoming, 2019.
9. A. K. Burrell, T. M. McCleskey, P. Shukla, H. Wang, T. Durakiewicz, D. P. Moore, C. G. Olson, J. J. Joyce, and Q. Jia, *Controlling Oxidation States in Uranium Oxides through Epitaxial Stabilization*, Adv. Mater. **19**, 3559–3563, 2007.
10. A. R. Fox, S. C. Bart, K. Meyer, and C. C. Cummins, *Towards uranium catalysts*, Nature **455**, 341–349, 2008.
11. G. J. Hutchings, C. S. Heneghan, I. D. Hudson, and S. H. Taylor, *Uranium-oxide-based catalysts for the destruction of volatile chloro-organic compounds*, Nature **384**, 341–343, 1996.
12. T. T. Meek and B. von Roedern, *Semiconductor devices fabricated from actinide oxides*, Vacuum **83**, 226–228, 2008.
13. Z. Sofer, O. Jankovsky, P. Simek, K. Klimova, A. Mackova, and M. Pumera, *Uranium- and Thorium-Doped Graphene for Efficient Oxygen and Hydrogen Peroxide Reduction*, ACS Nano **8**, 7106–7114, 2014.
14. S. W. Zhang, *Green tribology: fundamentals and future development*, Friction **1**, 186–194, 2013.
15. K. Holmberg, P. Andersson, and A. Erdemir, *Global energy consumption due to friction in passenger cars*, Tribol. Int. **47**, 221–234, 2012.
16. A. R. Konicek, D. S. Grierson, A. V. Sumant, T. A. Friedmann, J. P. Sullivan, P. U. P. A. Gilbert, W. G. Sawyer, and R. W. Carpick, *Influence of surface passivation on the friction and wear behavior of ultrananocrystalline diamond and tetrahedral amorphous carbon thin films*, Phys. Rev. B **85**, 155448, 2012.
17. J.-M. Martin, M.-I. De Barros Bouchet, C. Matta, Q. Zhang, W. A. Goddard III, S. Okuda, and T. Sagawa, *Gas-phase lubrication of ta-C by glycerol and hydrogen*

- peroxide. *Experimental and computer modeling*, J. Phys. Chem. C **114**, 5003–5011, 2010.
18. M.-I. De Barros Bouchet, G. Zilibotti, C. Matta, M. C. Righi, L. Vandenbulcke, B. Vacher, and J.-M. Martin, *Gas-phase lubrication of ta-C by glycerol and hydrogen peroxide. Experimental and computer modeling* Friction of diamond in the presence of water vapor and hydrogen. *Coupling gas-phase lubrication and first-principles studies*, J. Phys. Chem. C **116**, 6966–6972, 2012.
 19. G. Zilibotti, S. Corni, and M. C. Righi, *Load-induced confinement activates diamond lubrication by water*, Phys. Rev. Lett. **111**, 146101, 2013.
 20. L. Pastewka, S. Moser, P. Gumbsch, and M. Moseler, *Anisotropic mechanical amorphization drives wear in diamond*, Nat. Mater. **10**, 34–38, 2011.
 21. T. Kunze, M. Posselt, S. Gemming, G. Seifert, A. R. Koniczek, R. W. Carpick, L. Pastewka, and M. Moseler, *Wear, plasticity and rehybridization in tetrahedral amorphous carbon*, Tribol. Lett. **53**, 119–126, 2014.
 22. G. Moras, A. Klemenzenz, T. Reichenbach, A. Gola, H. Uetsuka, M. Moseler, and L. Pastewka, *Shear melting of silicon and diamond and the disappearance of the polyamorphic transition under shear*, Phys. Rev. Mater. **2**, 083601, 2018.
 23. T. Kuwahara, G. Moras, and M. Moseler, *Friction regimes of water-lubricated diamond (111): role of interfacial ether groups and tribo-induced aromatic surface reconstructions*, Phys. Rev. Lett. **119**, 096101, 2017.
 24. T. Kuwahara, G. Moras, and M. Moseler, *Role of oxygen functional groups in the friction of water-lubricated low-index diamond surfaces*, Phys. Rev. Mater. **2**, 073606, 2018.
 25. T. Kuwahara, P. A. Romero, S. Makowski, V. Weihnacht, G. Moras, and M. Moseler, *Mechano-chemical decomposition of organic friction modifiers with multiple reactive centres induces superlubricity of ta-C*, Nat. Commun. **10**, 151, 2019.